

QMF5 Fig. 3. Calculated trap potential as a function of the distance from the surface of the tip. The potential is normalized by the natural linewidth energy of a Rb atom.

the other hand, the signal in the region of more than 100 nm contains the far-field component. The intensity distribution in the near-field region is fitted with an exponential function of $I(r) = \exp(-0.84r/a)$, where a is a radius of aperture and r is the distance from the surface of the tip. The decay length of the near-field component is comparable to the aperture size a .

It has been proposed that an atom can be trapped at a minimum point of a trap potential composed of the repulsive dipole force and the attractive van der Waals force in a certain condition.^{4,5} To generate a stable trap potential for a Rb atom, we must pay attention to several parameters: van der Waals force, de Broglie wavelength and radius of the aperture. Here, in order to estimate the near-field optical potential for a Rb atom, we assume that the experimentally obtained function $I(r)$ can be applied to the case where the tip radius is smaller than 80 nm. When we consider the case of the optical near field power of 80 W/cm^2 and the frequency detuning of $\delta/2\pi$ of +1 GHz, we find the optimal trap potential can be formed if $a = 10 \text{ nm}$. In this case, the minimum point of the potential is found at a distance 60 nm from the surface of the tip, as shown in Fig. 3. The atom can be trapped at one of the quantized vibrational levels with n , drawn with horizontal line in the trap potential. When we regard the trap potential as a harmonic potential, the minimum level with $n = 0$ corresponds to the kinetic energy of $30 \text{ } \mu\text{K}$ in terms of the temperature. This temperature correspond to the de Broglie wavelength of 90 nm. If $a \geq 10 \text{ nm}$, the trap potential become too shallow to trap a Rb atom by conventional laser cooling technique. On the other hand, if $a \leq 10 \text{ nm}$, van der Waals force become dominant, and the trap potential disappears.

*Tokyo Inst. of Tech., Japan

**Tokyo Inst. of Tech. and Kanagawa Academy of Science and Tech., Japan

[†]Japan Science and Tech. Corp., Tokyo Inst. of Tech. and Kanagawa Academy of Science and Tech., Japan

1. J.P. Dowling and J. Gea-Banacloche, "Evanescent light-wave atom mirrors, resonators, waveguides, and traps," in *Advances in atomic, molecular, and optical physics*, B. Bederson and H. Walther, eds., Vol. 37 (Academic Press, San Diego, 1996), pp. 1–94.
2. M. Ohtsu, S. Jiang, T. Pangaribuan, M. Kozuma, "Nanometer resolution photon STM and single atom manipulation," in *Near-Field Optics*, D.W. Pohl and D. Courjon, eds. (Kluwer, Dordrecht, 1993), pp. 131–139.

3. H. Hori, "Quantum optical picture of photon STM and proposal of single atom manipulation," in *Near-Field optics*, D.W. Pohl and D. Courjon, eds. (Kluwer, Dordrecht, 1993), pp. 131–139.
4. H. Ito, K. Otake, M. Ohtsu, "Near-field optical guidance and manipulation of atoms," in *Far- and Near-Field optics*, (Society of Photo-Optical Instrumentation Engineers, Washington, 1998).
5. M. Ohtsu, eds., in *Near-field nano/atom optics and technology* (Springer-Verlag, Berlin, 1998).
6. T. Yatsui, M. Kourogi, M. Ohtsu, "Increasing throughput of a near-field optical fiber probe over 1000 times by the use of a triple-tapered structure," *Appl. Phys. Lett.* **73**, 2090–2092 (1998).

QMF6

11:30 am

Mapping the phase of light in an integrated optical waveguide device

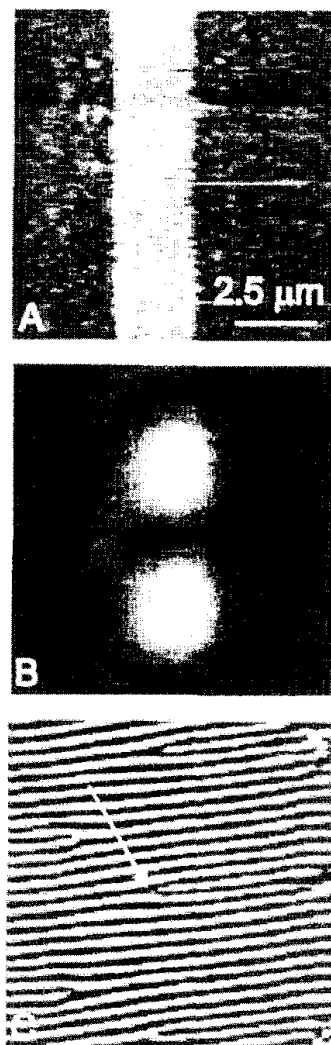
M.L.M. Balistreri, J.P. Korterik, L. Kuipers, N.F. van Hulst, *Applied Optics Group, MESA⁺ Research Inst. and Department of Applied Physics, Univ. of Twente, P.O. Box 217, 7500 AE Enschede, The Netherlands; E-mail: l.kuipers@tn.utwente.nl*

Nowadays, a measurement of the intensity of the optical field in integrated optical waveguide devices with a photon scanning tunneling microscope (PSTM) is reasonably routine.^{1–3} However, if one could visualize the evolution of the phase of the light field in real-space, it would yield new and detailed information concerning the properties of wavelength multiplexers, mode converters, etc., of which the operation depends critically on the phase of the light. Here, we believe we present the first phase maps of light in integrated optical waveguides obtained with a heterodyne interference PSTM.

A PSTM is based on the principle of frustration of the evanescent field at an air-waveguide interface when a coated optical fiber tip is brought in the near-field (a few nanometers) of this interface.^{1–3} The nonpropagating evanescent wave is locally converted into a propagating wave and guided through the fiber.

Maps of the relative phase of the optical field have been recorded by including the PSTM in one branch of a Mach-Zehnder interferometer. The photon-tunneling signal and the reference signal interfere in a 3dB-fiber coupler and this interference signal is detected with a photon multiplier tube. Acousto-optic heterodyne detection of the phase with a frequency of 40 kHz is used to detect the photon-tunneling signal. Through the use of both the in- and out-of-phase outputs of a lock-in amplifier, we can calculate the (cosine of the) phase and the amplitude of the optical field in the waveguide. By raster scanning the tip over the waveguide a phase map is obtained.

Figure 1 shows a phase measurements of a light ($\lambda = 632.8 \text{ nm}$) in a channel waveguide. Linear polarized light has been coupled in a controlled way in the input facet of the waveguide in order to simultaneously excite both TE_{00} and TM_{00} modes. The topography is shown in Fig. 1(a), the amplitude and the



QMF6 Fig. 1. Interferometric PSTM measurement of a Si_3N_4 channel waveguide. The width and the height step of the waveguide are $2.86 \text{ } \mu\text{m}$ and 4.2 nm , respectively. (a) Measured topographical image. (b) The measured amplitude of the optical field of the modes inside the waveguide. (c) The measured evolution of the cosine of the phase of the optical field. The arrow indicates a phase singularity.

phase of the optical field in Fig. 1(b) and 1(c), respectively. With the PSTM both TE- and TM polarized light is detectable.³ As a result, two modes with orthogonal polarization produce a detectable beating pattern. This pattern is observed in the amplitude map of Fig. 1(b). Surprisingly, the phase image contains phase singularities at various positions [indicated with the arrow in Fig. 1(c)].

The first phase measurements of the optical field in integrated optical waveguides have been performed with an interferometric PSTM. Because of so-called mode beating the phase exhibits singularities. Calculations show that these singularities occur at locations where the amplitudes of the modes are exactly equal and the modes are exactly out-of-phase.

1. A.G. Choo, H.E. Jackson, U. Thiel, G.N. De Brabander, J.T. Boyd, *Appl. Phys. Lett.* **65**, 947 (1994).

2. Y. Toda, and M. Ohtsu, IEEE Photon. Techn. Lett. 7, 84 (1995).
3. M.L.M. Balistreri, D.J.W. Klunder, J.P. Kortarik, F.C. Blom, A. Driessen, H.W.J.M. Hoekstra, L. Kuipers, N.F. van Hulst, Opt. Lett. in press (Dec. 1999).

QMF7

11:45 am

Near-field spectroscopy of surface excitations

K. Joulain, R. Carminati, J.-J. Greffet, A.V. Shchegrov,* *Laboratoire EM2C, Ecole Centrale Paris, Centre National de la Recherche Scientifique, 92295 Châtenay-Malabry Cedex, France; E-mail: remi@em2c.ecp.fr*

Correlations and spectral properties of thermal light have been the subject of many studies since the development of statistical optics and modern coherence theory.^{1,2} In most of the studies, the nonradiating (near field) part of the emitted light is disregarded, because it plays no role in the far-field emission properties of planar sources. Nevertheless, recent interest in microscale and nanoscale radiative transfer,³ together with the development of local-probe thermal microscopy⁴ and the observation of coherent thermal emission from doped silicon and silicon carbide (SiC) gratings,⁵ have raised new challenges. In fact, all these topics have in common the substantial role of the non-radiating (evanescent) thermal fields.

Spatial correlations of the near field thermally emitted by a planar opaque surface were studied recently.⁶ The strong influence of the non-propagating components of the field was put forward. In particular, it was shown that resonant surface excitations (surface-plasmon or surface-phonon polaritons) lead to long-range spatial correlations.⁶ This phenomenon is at the origin of spatially-coherent thermal emission of doped silicon and SiC gratings.⁵

In this work, we concentrate on the *spectral properties* of the thermally emitted near field. Our approach is based on fluctuational electrodynamics and the fluctuation-dissipation theorem.² The basic quantity to compute is the cross-spectral density tensor of the electric field:

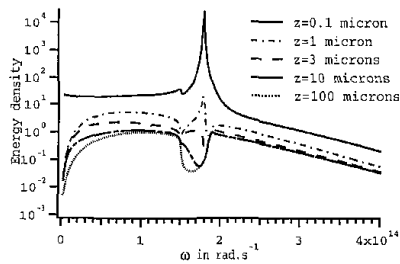
$$\langle E_j(\mathbf{r}_1, \omega) E_k^*(\mathbf{r}_2, \omega') \rangle = W_{jk}(\mathbf{r}_1, \mathbf{r}_2, \omega) \times \delta(\omega - \omega'), \quad (1)$$

where $E(\mathbf{r}, \omega)$ is the time-domain Fourier transform of the electric field and the brackets denotes an average over the ensemble of realizations of the field. The electric energy density is obtained by:

$$U_e(\mathbf{r}, \omega) = \frac{\epsilon_0}{2} \sum_j W_{jj}(\mathbf{r}, \mathbf{r}, \omega). \quad (2)$$

The method leads to an exact expression of the energy density $U_e(\mathbf{r}, \omega)$, which is valid in both near field and far field. In particular, the role of the interface and the existence of surface electromagnetic modes is taken into account.

We show that near-field excitations dramatically influence the spectrum of the emitted radiation. For example, we study a SiC surface in the infrared part of the spectrum. The energy density has a spectrum which changes strongly during the transition from the near field to the far field



QMF7 Fig. 1. Normalized near-field spectrum in a plane at a constant distance z from a planar SiC surface.

(Fig. 1). The near-field spectrum is a signature of the excitation of surface-phonon polaritons at wavelengths around $\lambda = 11, 3 \mu\text{m}$. We show that the features of this spectrum can be interpreted using the density of states of the surface modes.⁷

This work provides a powerful tool to describe near-field spectroscopic effects in thermal emission of light. Due to the possibility of measuring near-field spectra by using near-field optics techniques, this work could find applications in solid-state spectroscopy. It should also be helpful in modeling nanoscale radiative transfer of energy, where transfer through non-radiating modes is of fundamental importance.

*Univ. of Rochester, USA

1. L. Mandel and E. Wolf, *Optical Coherence and Quantum Optics* (Cambridge Univ. Press, Cambridge, 1995).
2. S.M. Rytov, Yu.A. Kravtsov, V.I. Tatarskii, *Principles of Statistical Radiophysics* (Springer-Verlag, Berlin, 1989), vol. 3, chap. 3.
3. C.L. Tien and G. Chen, J. Heat Transfer **114**, 799 (1994).
4. C.C. Williams and H.K. Wickramasinghe, Appl. Phys. Lett. **49**, 1587 (1986).
5. P.J. Hesketh *et al.*, Nature (London) **324**, 549 (1986); Phys. Rev. B **37**, 10,803 (1988); J. Le Gall *et al.*, Phys. Rev. B **55**, 10,105 (1997).
6. R. Carminati and J.-J. Greffet, "Near-field effects in spatial coherence of thermal sources," Phys. Rev. Lett. **82**, 1660 (1999).
7. A.V. Shchegrov, K. Joulain, R. Carminati, J.-J. Greffet, "Near-field spectroscopy of surface excitations," submitted for publication.

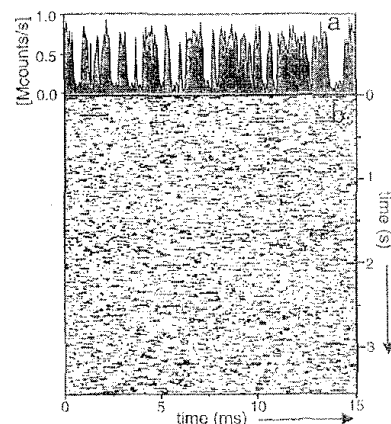
QMF8

NOON

Quantum jumps of individual emitters in a heterogeneous environment studied by near-field optics

Niek F. van Hulst, Joost-Anne Veerman, Maria F. Garcia-Parajo, L. (Kobus) Kuipers, *Applied Optics Group, Applied Physics, MESA+ Research Inst., Univ. of Twente, P.O. Box 217, 7500 AE Enschede, The Netherlands; E-mail: N.F.vanHulst@tn.utwente.nl*

We have performed real-time and orientation resolved measurements of single fluorescent molecules (DiIc₁₈) in thin films of PMMA and polystyrene at ambient and reduced oxygen conditions. Fluorescent time trajectories of single molecules have been recorded using a



QMF8 Fig. 1. (a) Single molecule fluorescence timetrace with 57 μs integration time per point. The fluorescence drops repeatedly to a low level due to transitions to T_1 . (b) Image with 3.5 s of fluorescence blinking. The gray level represents the photon count rate during a 57 μs bin; bright streaks are due to S_0-S_1 cycling; dark streaks represent residence in the triplet state.

two-channel near-field optical microscope,¹ with 30- μs real-time resolution.

A typical fluorescence trajectory is shown in Fig. 1, covering 3.5 sec with 5 orders of magnitude dynamic range. Real-time singlet-triplet jumps (S_1-T_1) are directly observed.

We find that both triplet state lifetime and crossing yield vary in time due to the local heterogeneity of the polymeric host.^{2,3} A triplet lifetime distribution, both in space and in time, is constructed from the data. The triplet lifetime distribution for PMMA peaks at 180 μs with 130 μs FWHM, as compared to 50 μs , 20 μs FWHM, for polystyrene. The main cause is a difference in oxygen solubility and mobility, as confirmed by varying the oxygen concentration of the sample. Within the triplet lifetime we determine an average number of collisions with oxygen of 3 and 11 for PMMA and polystyrene, respectively.

The inter-system crossing yield appear to be hardly correlated to the triplet lifetime, with only weak effect of the presence of oxygen.

Photo-dissociation occurs after emitting 10^6 or 10^7 photons typically for PMMA and polystyrene, respectively. Dissociation due to singlet oxygen would be most likely. Yet, again the dissociation probability shows no correlation with triplet lifetime or inter-system crossing yield for either of the investigated environments, in contrast to other observations.⁴

Finally discrete rotational jumping between two conformationally defined orientations is observed.

New insight in the photo-dynamics and orientational mobility of individual molecules is obtained using single molecule detection: time-varying heterogeneity, correlations and distributions of photo dynamic parameters.

1. A.G.T. Ruiter, J.A. Veerman, M.F. Garcia-Parajo, N.F. van Hulst, J. Phys. Chem. A **101**, 7318 (1997).
2. T. Basché, W.E. Moerner, M. Orrit, U.P. Wild, (eds.) *Single-Molecule Optical Detection, Imaging and Spectroscopy*, (VCH, Weinheim, 1997).